Cascaded Emission from a Dual-Wavelength Quantum Cascade Laser

Kale J. Franz, Daniel Wasserman, Anthony J. Hoffman, and Claire Gmachl
Department of Electrical Engineering, Princeton University, Princeton, NJ 08544 USA
Author email address: kfranz@princeton.edu

Kuen-Ting Shiu and Stephen R. Forrest
Dept. of Electrical Engineering & Dept. of Physics, University of Michigan, Ann Arbor, MI 48109 USA

Abstract: We present evidence for "cascaded" laser emission in Quantum Cascade lasers, demonstrating a dual wavelength (~9.6 μm and ~8.2 μm) laser with two consecutive optical transitions in each active region.

OCIS codes: (140.5960) Semiconductor lasers; (140.3070) Infrared and far-infrared lasers

1. Introduction

The inherent design flexibility of Quantum Cascade (QC) emitters has led to unique laser concepts that have revolutionized mid-infrared light sources [1]. Several innovative designs have focused on multi-wavelength QC devices [2-4]. One approach, while unsuccessful, attempted stacked optical transitions for a so-called "cascaded" QC laser [2]. Such a laser would be of interest for cascaded optical transitions that produce correlated photons, which have been demonstrated in other laser systems [5]. Here we report a dual-wavelength QC laser that shows simultaneous lasing from two cascaded optical transitions in its active regions.

2. Laser design and fabrication

Our dual-wavelength design is based on two consecutive "cascaded" optical transitions in each QC active region. The upper optical transition at 9.6 μm is composed of a second-excited state and first-excited state of the constituent quantum wells of a two-well QC active region. The lower optical transition at 8.2 μm results from a first-excited to ground state transition.

The laser was grown by gas source molecular beam epitaxy with InGaAs/InAlAs quantum wells lattice-matched to an InP:S substrate (doped $n < 2\times10^{17}$ cm^{-3}). Forty active-injector periods were used for the active core, which was clad above and below by 0.55 μm of InGaAs ($n = 5\times10^{16}$ cm^{-3}). Additional top cladding layers of 3.9 μm InP ($n = 5\times10^{16}$ cm^{-3}) and 1.1 μm InP ($n = 6.7\times10^{18}$ cm^{-3}) were grown. Following growth, we post-calibrated layer thicknesses, and the as-grown band structure is shown in Fig. 1(a). Lasers were processed using a standard procedure as in Ref. [3]. The waveguide loss is estimated at 7.4 cm^{-1} for $\lambda = 9.6$ μm and 5.1 cm^{-1} for $\lambda = 8.2$ μm. The optical confinement factor for the active core is 60% and 67% for the two wavelengths, respectively, with optical dipole matrix elements $z_{54} = 31$ Å and $z_{42} = 14$ Å.

3. Device testing and analysis

Time-integrated laser spectra for increasing electric field and current density are shown in Fig. 1(b). We observe laser action at $\lambda \sim 9.3$ μm and $\lambda \sim 8.2$ μm. With increasing field, the spectral distance between the two laser lines decreases. We

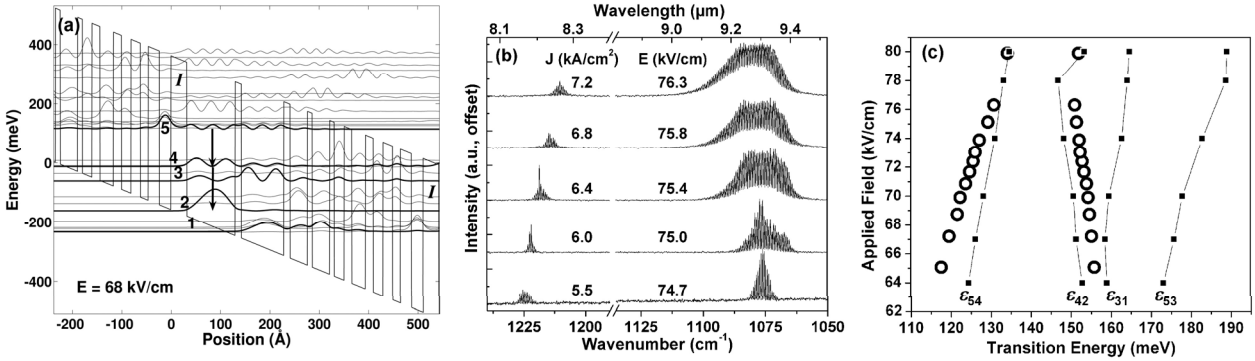

Fig. 1. (a) Conduction band diagram of one active region between two injector regions. Cascaded optical transitions are between levels 5 & 4 and 4 & 2. A single stage of the layer sequence is (in angstroms starting from the injection barrier ***I***) **40**/100/**16**/88/**16**/36/**12**/36/**12**/20/**20**/28/**20**/20/**24**/16/**28**/24, where InAlAs barriers are in bold, InGaAs wells are in normal font, and Si-doped (2×10^{17} cm^{-3}) layers are underlined. (b) Emission spectra from a 2.5 mm long and 10 μm wide laser at a heat sink temperature of 80 K with a 47 ns current pulse width. (c) Measured and calculated values of the optical transition energies in electroluminescence (EL) in relation to applied electric field. Hollow circles represent the center points of multi-Lorentzian fits to the EL the data. For a given field, squares show the calculated transition energies.

also examined electroluminescence (EL) spectra from deep-etched semicircular mesas, and found two prominent optical transitions centered near 9.6 μm and 8.2 μm that decrease in spectral separation with increasing field. Electroluminescence data are displayed in Fig. 1(c), represented by two series of open circles. Overlaid on Fig. 1(c) are calculated transition energies. The energies and field behavior of the emission are consistent with calculations for the 5→4 and 4→2 cascaded transitions. No other combination of optical transitions can fully account for the experimentally observed behavior. Furthermore, the ~9.6 μm transition has a relatively broad EL spectrum (18.7 meV), compared to the more narrow ~8.2 μm transition (16.2 meV). This suggests a diagonal and vertical transition, respectively, which is indeed the case for 5→4 and 4→2 transitions as confirmed by the Fig. 1(a) band structure.

Figure 2 displays light-current-voltage (LIV) data collected using a 14 ns boxcar gate at six positions within an 80 ns current pulse. A long-pass filter with cutoff at 8.6 μm was used to discriminate between the ~8.2 μm and ~9.6 μm light. While the two laser thresholds are very close, the ~9.6 μm light has a higher slope efficiency compared to the weaker ~8.2 μm laser line for $t = 0$. Later in the current pulse, the ~8.2 μm light overtakes the ~9.6 μm light in power. Also as the pulse progresses, the threshold of the ~9.6 μm light increases. The trend of less powerful ~9.6 μm light relative to the ~8.2 μm light is seen both with increasing pulse width (or gate position) and increasing temperature, suggesting the behavior is thermally induced. Non-radiative transition lifetimes are temperature dependent, with lifetimes decreasing as temperature increases [1]. Thus, level 4 populates more rapidly with increasing temperature, effectively reducing population inversion for the 5→4 transition while increasing inversion for the 4→2 transition.

That population inversion can occur for the 4→2 transition may not be immediately obvious. In our structure, however, we have circumstances similar to those reported in Ref. [6], where local population inversion in *k*-space is achieved for a single quantum well active region, while global population inversion is not necessary. For the 4→2 transition in our device, an electron that non-radiatively scatters to state 2 must scatter at least four more times before it affects local population inversion at the laser transition. As in Ref. [6], there are furthermore many injector states near state 2 into which electrons higher in the band can tunnel, so 4→2 population inversion is also made possible by the emptying of state 2 through tunneling.

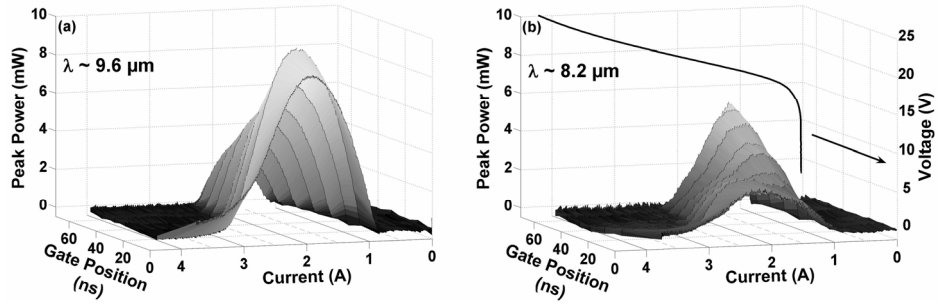

Fig. 2. Gated light vs. current plots for (a) λ ~ 9.6 μm and (b) λ ~ 8.2 μm. The graphs show data from a 14 ns gate with rising edge positioned at 0, 10, 20, 30, 40, 50, 60, and 66 ns throughout an 80 ns current pulse. The 40 ns current vs. voltage curve is also shown in (b).

4. Conclusions

We have presented a dual-wavelength (~9.6 μm and ~8.2 μm) QC laser that exhibits simultaneous emission from two cascaded optical transitions in each QC active region. This is believed to be the first demonstration of a "cascaded" QC laser.

5. Acknowledgements

This work was supported in part by MIRTHE (NSF-ERC) and DARPA-LPAS. K.J.F. gratefully acknowledges the support of the National Science Foundation Graduate Research Fellowship Program.

6. References

[1] C. Gmachl, F. Capasso, D. L. Sivco, and A. Y. Cho, "Recent progress in quantum cascade lasers and applications," *Rep. Prog. Phys.*, vol. 64, pp. 1533-1601, 2001.

[2] C. Sirtori, A. Tredicucci, F. Capasso, J. Faist, D. L. Sivco, A. L. Hutchinson, and A. Y. Cho, "Dual-wavelength emission from optically cascaded intersubband transitions," *Opt. Lett.*, vol. 23, pp. 463-465, 1998.

[3] C. Gmachl, A. Belyanin, D. L. Sivco, M. L. Peabody, N. Owschimikow, A. M. Sergent, F. Capasso, and A. Y. Cho, "Optimized second-harmonic generation in quantum cascade lasers," *IEEE J. Quantum Electron.*, vol. 39, pp. 1345-1355, 2003.

[4] A. Tredicucci, C. Gmachl, F. Capasso, D. L. Sivco, A. L. Hutchinson, and A. Y. Cho, "A multiwavelength semiconductor laser," *Nature*, vol. 396, pp. 350-353, 1998.

[5] H. J. G. a. P. V. Goedertier, "A Gaseous (He-Ne) Cascade Laser," *Appl. Phys. Lett.*, vol. 4, pp. 20-21, 1964; M. O. Scully, "Correlated Spontaneous-Emission Lasers: Quenching of Quantum Fluctuations in the Relative Phase Angle," *Phys. Rev. Lett.*, vol. 55, pp. 2802-2805, 1985.

[6] J. Faist, F. Capasso, C. Sirtori, D. L. Sivco, A. L. Hutchinson, M. S. Hybertsen, and A. Y. Cho, "Quantum Cascade Lasers without Intersubband Population Inversion," *Phys. Rev. Lett.*, vol. 76, pp. 411-414, 1996.